



PERGAMON

SCIENCE @ DIRECT®

Radiation Physics and Chemistry ■ (■■■■) ■■■-■■■

Radiation Physics  
and  
Chemistry[www.elsevier.com/locate/radphyschem](http://www.elsevier.com/locate/radphyschem)

# Theoretical evaluation of granular scintillators quantum gain incorporating the effect of K-fluorescence emission into the energy range from 25 to 100 keV

I. Kandarakis<sup>a,\*</sup>, D. Cavouras<sup>a</sup>, E. Ventouras<sup>a</sup>, C. Nomicos<sup>b</sup>

<sup>a</sup> Department of Medical Instruments Technology, Technological Educational Institution of Athens, Ag. Spyridonos Street, Egaleo, 122 10 Athens, Greece

<sup>b</sup> Department of Electronics, Technological Educational Institution of Athens, Ag. Spyridonos Street, Egaleo, 122 10 Athens, Greece

Received 30 April 2002; received in revised form 25 September 2002; accepted 5 November 2002

## Abstract

A theoretical study on optical quantum gain of granular scintillators used in detectors of medical imaging systems is presented. The fraction of optical gain due to K-characteristic radiation was also determined. The study was applied on two widely known scintillating materials, Gd<sub>2</sub>O<sub>2</sub>S:Tb and ZnSCdS:Ag, for various incident photon energies and scintillator coating thickness. Optical quantum gain due to K-characteristic photons varies with incident photon energy and scintillator coating thickness and may amount to up to 20% or 29% for Gd<sub>2</sub>O<sub>2</sub>S:Tb and ZnSCdS:Ag respectively. © 2003 Elsevier Science Ltd. All rights reserved.

**Keywords:** X-ray imaging; Scintillators; Radiation detectors; X-ray luminescence

## 1. Introduction

During the past several decades a large number of new scintillating materials have been experimentally investigated and employed in radiation detectors used in various fields of research. In medical imaging, interest in studying the intrinsic scintillator properties of materials has been renewed due to the wide use of novel digital imaging detectors (Yaffe and Rowlands, 1997; Besch, 1998; Hell et al., 2000; Ning et al., 2000). These detectors are principally based on scintillators coupled to CCD or amorphous silicon TFT arrays. In most medical applications, the choice of detector material is crucial, since it may significantly affect patient radiation dose and image diagnostic value. In this sense, a factor of primary importance, which determines the detector output signal, is the detector optical quantum gain

(DOG). DOG is the gain of the detection process expressed in number of photons (quanta), e.g. number of final photons (optical quanta emitted by the scintillator) per initial photon (incident radiation photon). The quantum detection efficiency or quantum efficiency which is the fraction of absorbed radiation quanta primarily determines DOG. This fraction depends on the energy of incident photons, the atomic composition of the scintillator and on the scintillator thickness. An additional important factor is the energy of the K-absorption edge for photoelectric interactions. For photon energies exceeding this K-edge energy, a fraction of the absorbed radiation is re-emitted in the form of characteristic X-ray fluorescence. For various radiation detection problems and imaging applications employing photons in the range between 20 and 100 keV, this effect may be significant and may seriously affect detector performance.

Additional factors of equal importance for the detection process are: (1) the intrinsic conversion efficiency, i.e. the efficiency of the material to convert

\*Corresponding author. Tel.: +30-10-5385-375; fax: +30-10-5910-975.

E-mail address: [kandarakis@teiath.gr](mailto:kandarakis@teiath.gr) (I. Kandarakis).

incident radiation into light, and (2) the attenuation of this light during transmission to the output surface of the scintillator. The conversion of radiation is a function of the forbidden energy band gap between the valence and conduction bands and the type of activator introduced within the scintillator's crystal lattice. Activators create new energy states within the forbidden energy band gap which determine the wavelength of the emitted optical photons. The transmission of light through a scintillator depends on the optical properties of the material. Of special interest for medical imaging are scintillators in granular form, often called phosphors. This type of detector is widely used in projection X-ray imaging (radiography, fluoroscopy), in portal imaging with medical accelerators and also in some computed tomography detectors. Additional applications in nuclear research, in crystallography or in astrophysics have been reported (Phillips et al., 1993; Zurro et al., 1995). These scintillators consist of a layer containing active scintillating grains embedded in a non-active binding material. The presence of grains increases optical scattering effects resulting in significant light attenuation, especially for optical quanta laterally directed with respect to incident radiation. This effect, however, may ameliorate image spatial resolution and improve image quality.

The aim of the present study was to develop a model for detector optical quantum gain of granular scintillators incorporating the following: (1) the effect of K X-ray fluorescence emission and re-absorption, (2) the dependence of the intrinsic radiation to light conversion process on inherent material properties, e.g. forbidden energy band gap, optical photon energy determined by energy state modifications caused by activators, and (3) the optical attenuation effects: scattering, absorption and reflectivity.

Previously published theoretical calculations study the effects of X-ray fluorescence (Chan and Doi, 1983), the optical properties (Hamaker, 1947; Ludwig, 1971; Swank, 1973; Nishikawa and Yaffe, 1990; Lindström and Carlsson, 1999), the inherent quantum and crystal lattice properties related to the intrinsic radiation to light conversion process (Blasse, 1994; Bartram and Lempicki, 1996). The present study, however, is extended to include all the aforementioned effects in one model and uses experimental data obtained on laboratory prepared test scintillator layers.

## 2. Method

### 2.1. Optical quantum gain without account of K-fluorescence emission

The detector optical quantum gain  $G_\Lambda$  of an irradiated scintillator layer may be defined by the following

equation:

$$G_\Lambda(E, L) = \bar{\eta}(E, L) \bar{\phi}_\Lambda(E, \lambda) \quad (1)$$

with  $\bar{\eta}$ , the mean quantum efficiency, expressing the fraction of incident radiation quanta absorbed by the scintillator,  $E$  the energy of an incident photon, and  $L$  the thickness of the layer.  $\bar{\phi}_\Lambda$  is the mean optical quantum conversion gain, accounting for the number of optical quanta created within the mass of the scintillator and escaping the scintillator per radiation photon absorbed.

Quantum efficiency is determined by the absorption coefficient and thickness of the scintillator layer and may be calculated by considering exponential absorption of the incident radiation. Absorption coefficients may be calculated from tabulated data using the sum of absorption coefficients of the chemical elements contained in the scintillator material, weighted by the corresponding atomic weight (Storm and Israel, 1967; Hubbell and Seltzer, 1995). The coefficient used in the calculations of this section was the mass-energy absorption coefficient ( $\mu_{\text{en}}/\rho$ ) (Hubbell et al., 1969; Hubbell, 1999), also denoted as  $(\mu/\rho)_{\text{tot, en}}$ , e.g. total mass-energy absorption coefficient (Storm and Israel, 1967; De Porter and Bril, 1975). This coefficient takes into account all the modes of energy transfer from primary incident radiation quanta to secondary electrons (photoelectrons, Compton recoil electrons, etc.) in the absorbing material. However, it also assumes loss of all secondary photons created just after the primary interaction effect, i.e. it does not take into account the creation and re-absorption of: (i) K-characteristic fluorescence X-rays, (ii) coherently or incoherently scattered photons, (iii) bremsstrahlung and (iv) annihilation photons (Hubbell and Seltzer, 1995; Hubbell, 1999). Hence, the effect of radiation absorption is underestimated. A correction for the K-fluorescence emission due to the photoelectric effect will be given in the next section. Considering the effective atomic number of most currently employed scintillator materials, this effect is the most likely photon interaction in the medical diagnostic energy range (Evans, 1955; Knoll, 1989). A related coefficient is the mass absorption coefficient  $((\mu/\rho)_a$  or  $(\mu/\rho)_{\text{tot, a}}$ ), which assumes that K-fluorescence photons are totally absorbed within the volume of interest (De Porter and Bril, 1975; Hubbell, 1999). Hence, a corresponding correction is also necessary in situations in which  $(\mu/\rho)_a$  is applied.

The optical quantum conversion gain,  $\bar{\phi}_\Lambda$ , may be given in terms of the intrinsic radiation to light conversion efficiency  $\eta_C$ , expressing the fraction of absorbed radiation energy that is converted into light within the scintillator (Ludwig, 1971):

$$\bar{\phi}_\Lambda(E, \lambda) = \frac{\bar{\eta}_C E}{\hbar\omega} \bar{\Phi}_\Lambda(\lambda), \quad (2)$$

where  $\hbar\omega$  denotes the mean energy of an optical photon. The ratio  $(\bar{\eta}_C E/\hbar\omega)$  gives the number of optical photons initially created within the mass of the scintillator material following the absorption of one incident radiation photon.  $\Phi_\Lambda$  is the light transmission efficiency, providing for the fraction of initial optical photons  $(\bar{\eta}_C E/\hbar\omega)$  that escape to the output surface of the scintillator. The intrinsic conversion efficiency  $\eta_C$  is inversely proportional to the forbidden energy band gap ( $E_G$ ) between the valence energy band and the conduction energy band of the scintillator material (Alig and Bloom, 1977; Blasse, 1994). The average energy that must be transferred by the secondary electron (e.g. photoelectron) to create an electron–hole pair in the scintillator is approximately equal to  $\beta E_G$ , with  $\beta$  being a constant characterizing the excess energy above  $E_G$  that should be absorbed for an electron–hole pair to be created. For most materials  $\beta$  is approximately equal to 3 or slightly higher (Alig and Bloom, 1977; Blasse, 1994). However, the use of ion activators causes some modification of the energy bands resulting in less energy transitions and, hence, the emitted optical photon is of lower energy than the band gap in pure materials. Given that the secondary electron energy is totally absorbed, the value of the intrinsic conversion efficiency may be calculated by the relation (Blasse, 1994):

$$\eta_C = (\hbar\omega/\beta E_G)SQ \quad (3)$$

with  $S$  the electron–hole pair energy transfer efficiency that expresses the fraction of electron–hole pair energy transferred to the activator site, and  $Q$  the absorption efficiency of the activator site, expressing the fraction of transferred electron–hole pair energy absorbed at the activator site.  $S$  depends on (a) the complexity of the crystal structure of the scintillator, (b) the concentration of defects, and (c) the concentration of intentionally inserted impurities, which create the so-called impurity potential attracting electron–hole pairs (Blasse, 1994).  $Q$  depends on the intensity of crystal lattice vibrations and on the fraction of energy transferred to these vibrations. Normally,  $S$  and  $Q$  have values lower but close to unity. Since  $\hbar\omega < E_G$ , the intrinsic conversion efficiency is significantly lower than unity.

## 2.2. Optical quantum gain including K-fluorescence emission effect

When the incident photon energy just exceeds the K-photoelectric absorption edge, the incident radiation absorption shows a sudden increase. However, a fraction of the absorbed energy may be remitted from the scintillator in the form of K-fluorescence characteristic X-rays. The latter are produced at the sites of primary photon absorption and may either be re-absorbed at another site within the mass of the active

material or escape the scintillator. Scintillations (light bursts) will be generated at the sites of re-absorption.

In the present study, the effect of K-fluorescence characteristic rays on the optical quantum gain of scintillators has been taken into account as follows. The scintillator was assumed to be divided into a large number ( $I$ ) of elementary thin layers of thickness  $\Delta L$ . K-fluorescence rays were then assumed to be isotropically emitted from each point of primary radiation interaction, within a solid-angle element  $\Delta\Omega_j$ , where  $j = 1, 2, 3, \dots, J$  and  $J\Delta\Omega_j = 4\pi$ . The solid angle  $\Delta\Omega_j$  corresponds to the polar angle element  $\Delta\xi$  shown in Fig. 1.

The probability,  $p_{A,F}^L$ , of generation and absorption of a K-characteristic fluorescence photon, within the whole scintillator, may be calculated by a relation of the form (see Appendix A for details):

$$p_{A,F}^L(E_y) = \sum_{i=1}^I p_{Fy}^i(E, E_y) \sum_{e=1}^I \sum_{j=1}^J p_{A,j}^{i,e}(E_y, \Delta\Omega_j), \quad (4)$$

where  $p_{Fy}^i$  is the probability of generating a K-fluorescence photon in the  $i$ th layer of the scintillator, after the incidence of one radiation photon of energy  $E$  (Chan and Doi, 1983; Kalivas et al., 1999).  $p_{A,j}^{i,e}$  is the probability that a K-fluorescence X-ray photon, generated at the  $i$ th scintillator layer and emitted into a solid-angle element  $\Delta\Omega_j$ , interacts at the  $e$ th layer.  $E_y$  is the energy of the generated K-fluorescence photon. This photon may be either a  $K_\alpha$  or  $K_\beta$  fluorescence photon. The index  $y$  denotes either  $\alpha$  or  $\beta$ . In relation (4),  $p_{A,F}^L$  is obtained after summation over all the elementary thin layers  $i$  and  $e$  over the solid-angle elements  $j$ .

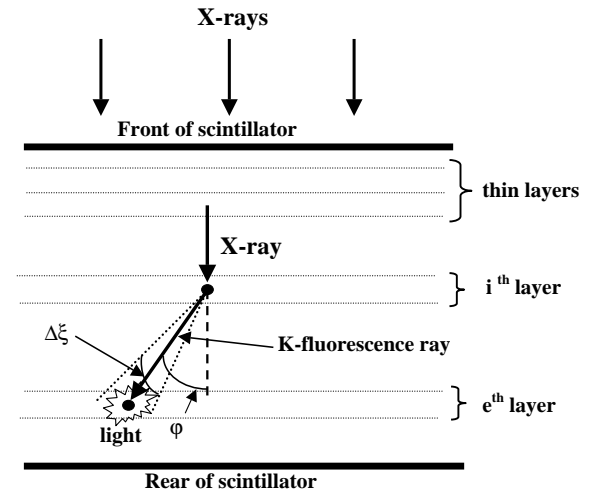


Fig. 1. Geometrical configuration for calculating K-fluorescence emission.

The optical quantum gain,  $G_{\Lambda}^K$ , of the scintillator, due to a K-fluorescence photon, may be expressed by the following equation:

$$G_{\Lambda}^K(E_y, L_0) = \sum_{i=1}^I p_{F_y}^i(E, E_y) \sum_{e=1}^I \sum_{J=1}^J p_{A,J}^{i,e}(E_y, \Delta\Omega_j) \times (\eta_C E_y / \hbar\omega) \bar{\Phi}_{\Lambda}^e(\lambda), \quad (5)$$

where  $(\eta_C E_y / 2\hbar\omega)$  is the number of optical quanta created within the whole scintillator after the absorption of one K-fluorescence X-ray photon, and  $\bar{\Phi}_{\Lambda}^e(\lambda)$  is the probability of each of these light photons escaping the scintillator (light transmission efficiency).

Finally, the total optical quantum gain of the scintillator may be given as the sum:

$$G_{\Lambda}^0(E, E_y, L_0) = G_{\Lambda}(E, L_0) + G_{\Lambda}^K(E_y, L_0), \quad (6)$$

where the first term corresponds to optical gain without K-fluorescence, given by Eq. (1).

### 2.3. Model for optical photon generation and transmission

The optical quantum conversion gain for granular form scintillators in the presence of, for example, optical scatterers may be determined by considering the radiative transfer theory, simplified by Swank's diffusion equation approximation (Swank, 1973; Groenhuis, et al., 1983; Ishimaru, 1989). Through the solution of this equation, the function  $\bar{\phi}_{\lambda}$  is obtained, giving the mean fraction of optical photons generated at depth  $i\Delta L$  which escape to the scintillator output surface per radiation photon absorbed. This fraction forms an optical pulse (scintillation) and this is given as a function of material optical properties (see Appendix A). Based on this solution the light transmission efficiency of the scintillator material may be expressed as follows:

$$\bar{\Phi}_{\Lambda}(\lambda) = \sum_{i=1}^I \bar{\phi}_Q(E, L_0) \bar{\phi}_{\lambda}(\sigma(\lambda), \tau(\lambda), L_0), \quad (7)$$

where the function  $\bar{\phi}_{\lambda}$  has been expressed in terms of the reciprocal optical diffusion length  $\sigma(\lambda)$  and the reciprocal optical relaxation length  $\tau(\lambda)$  (Swank, 1973). These two parameters have been expressed via the optical scattering ( $\lambda_S$ ) and optical absorption ( $\lambda_A$ ) coefficients which are functions of the optical wavelength  $\lambda$  as follows:

$$\sigma(\lambda) = [\lambda_A(\lambda^{-1})[\lambda_A(\lambda^{-1}) + 2\lambda_S(\lambda^{-n})]]^{1/2}, \quad (8a)$$

$$\tau(\lambda) = \lambda_A(\lambda^{-1}) + 2\lambda_S(\lambda^{-n}), \quad (8b)$$

where  $n$  depends on the optical scattering mechanism, being mainly Mie scattering (Van de Hulst, 1957; Morlotti 1975). Within granular scintillators, optical scattering is the main light attenuation mechanism. Hence,  $\lambda_S$  should be significantly higher than  $\lambda_A$  and,

accordingly  $\tau$ , which is principally affected by optical scattering, is higher than  $\sigma$ . Optical scattering also depends on the grain size and the complex index of refraction. However, these two parameters were assumed to be approximately equal for the materials considered in this study. This assumption was based on (a) grain size data found in manufacturer's data sheet (Lumilux Ltd.) and (b) refraction index values reported in literature and in manufacturers data sheet (values ranging between 2.36 and 2.6 for both materials) (Zweig and Zweig, 1983; Knoll, 1989; Lumilux Ltd, 1989). The two expressions in relations (8) have been obtained by combining the diffusion equation of Swank and the one-dimensional Hamaker–Ludwig model (Hamaker, 1947; Ludwig, 1971).

The function  $\bar{\phi}_Q$  in (7) gives the relative probability for an incident radiation photon to be absorbed at depth  $i\Delta L$ . The product of functions  $\bar{\phi}_{\lambda}$  and  $\bar{\phi}_Q$  gives the probability of an optical pulse being created at depth  $i\Delta L$  and arriving at the scintillator output surface. Summation over all thin scintillating layers  $\Delta L$  gives the probability of an optical pulse, generated anywhere within the scintillator mass, escaping at the output. This probability is the light transmission efficiency.

### 2.4. Input data and calculations

Data on X-ray coefficients and parameters related to K-fluorescence emission were obtained from the literature (Storm and Israel, 1967; Hubbell and Seltzer, 1995; Hubbell et al., 1994). The energy range was chosen to be between 25 and 100 keV. This is a useful range for a significant fraction of medical diagnostic applications. Most high voltage (kVp) imaging techniques, e.g. computed tomography or chest radiography, are also included in this range since, due to the spectral distribution of X-rays (Evans, 1955), a 150 kVp beam corresponds to a mean energy close to 100 keV. Additionally, within this range the effect of K-fluorescence is of most importance.

The values of optical scattering and optical absorption coefficients used in the calculations were estimated by fitting Eq. (1) to experimental gain data published in previous studies (Kandarakis et al., 1997; Kalivas et al., 1999a; Kandarakis and Cavouras, 2001a–c). The fitting technique was based on the Levenberg–Marquardt method (Bevington, 1969; Press et al., 1990). This was performed by allowing the values of  $\sigma$  and  $\tau$ , for optical scattering and optical absorption ( $\lambda_A$  and  $\lambda_S$ ), respectively, to vary. The value of the intrinsic radiation to light conversion efficiency ( $\eta_C$  in (2) and (3)) used in the calculations was determined by taking into account relation (3). During the fitting procedure  $\eta_C$  was kept constant. This can be considered a reasonable approach since the intrinsic conversion efficiency depends mainly on intrinsic parameters of rather fixed value, e.g. energy

band gap of the scintillator material, mean energy of light photons (Alig and Bloom, 1977; Blasse, 1994). Thus,  $\eta_C$  may be more or less accurately calculated using these fixed values. On the other hand, the light attenuation coefficients depend on statistically varying parameters, e.g. on the actual spatial, shape and size distribution of grains as well as on the wavelength spectral distribution. Consequently, the exact values of  $\lambda_A$  and  $\lambda_S$  may vary from point to point within the scintillator layer. Hence, only some measure of effective attenuation values, as is for instance those obtained by the fitting, may be macroscopically accepted as overall values which express the light attenuation properties of the whole scintillator layer.

All data presented in this study concern two particularly high performance scintillators, namely  $\text{Gd}_2\text{O}_2\text{S:Tb}$  and  $\text{ZnSCdS:Ag}$  having the following respective intrinsic physical properties: (1)  $\text{Gd}_2\text{O}_2\text{S:Tb}$  is a high density ( $7.4\text{ g/cm}^3$ ) high effective atomic number (59.5) scintillator. The K-absorption edge of Gd, being the highest atomic number element in the scintillator, is at 50.2 keV. The latter is well within the X-ray energy range employed in general-purpose X-ray imaging and therefore scintillator imaging performance may be significantly affected by secondary photon emission. It should be noted that the  $\text{Tb}^{3+}$  activator, having higher atomic number than Gd, is present in trace quantity only (approximately 0.3%), and its effect on radiation absorption is assumed to be negligible (Arnold, 1979; Curry et al., 1990). The energy band gap of  $\text{Gd}_2\text{O}_2\text{S}$  is relatively low ( $E_G = 4.5\text{ eV}$ ) and the optical emission spectrum, due to  $^5\text{D}_4 \rightarrow ^7\text{F}_J$  transitions of  $\text{Tb}^{3+}$  ions, corresponds to a mean optical photon energy of  $\hbar\omega = 2.4\text{ eV}$ . Additionally, the  $\text{Tb}^{3+}$  activator is easily oxidized resulting in high impurity potential. Thus, holes are efficiently collected at the activator site. This corresponds to high values of electron-hole energy transfer efficiency ( $S \approx 1$ ). Finally, absorption of hole-energy via large electron transitions (narrow line spectra) predominates in  $\text{Tb}^{3+}$  activated scintillators. This is because the coupling between electronic transitions and lattice vibrations is weak (Blasse, 1994). Thus, energy losses through lattice vibrations are minimized. As a result the electron-hole quantum efficiency is high ( $Q \approx 1$ ). This is apparent from the narrow line optical emission spectra of  $\text{Gd}_2\text{O}_2\text{S:Tb}$ . (2)  $\text{ZnSCdS:Ag}$  is a medium density ( $4.5\text{ g/cm}^3$ ) and medium effective atomic number (38.4) scintillator, the K-absorption edge of Cd, which is the highest atomic number element in the scintillator, is at a relatively low photon energy (26.7 keV). This affects scintillator performance when low energy soft tissue techniques are applied with the intent of enhancing image contrast, e.g. mammography, using tube voltages in the range 25–35 kVp. The presence of Ag activator, which is found at very low concentrations, does not affect the scintillator absorp-

tion properties. The energy band gap of  $\text{ZnSCdS}$  is low ( $E_G = 3.9\text{ eV}$ ) and the mean energy of the emitted optical photons is  $\hbar\omega = 2.75\text{ eV}$ .  $\text{ZnSCdS}$  has a rather medium-width band optical emission spectra (Kandarakis et al., 1997). This corresponds to high values of  $Q$  due to a transition-lattice vibration coupling of intermediate strength.

Based upon the aforementioned data ( $E_G = 4.5$  or  $3.9\text{ keV}$ ,  $\hbar\omega = 2.4$  or  $2.75\text{ eV}$ ,  $S = 1$ ,  $Q = 1$ ,  $\beta = 3$ ) and using relation (3), the intrinsic conversion efficiency was determined to be 0.19 for  $\text{Gd}_2\text{O}_2\text{S:Tb}$  and 0.22 for  $\text{ZnSCdS:Ag}$ . These values are slightly higher than those given by others (Arnold, 1979; Zweig and Zweig, 1983). However, they are close to our previously published data (0.20 and 0.224, respectively) (Kandarakis et al., 1997; Kandarakis and Cavouras, 2001a–c). Our results seem to be in good agreement with the estimation that values of  $Q$  and  $S$  are very close to unity for the two materials. The values of the optical attenuation coefficients, estimated by the fitting, were  $\sigma = 30\text{ cm}^2/\text{g}$  and  $\tau = 1000\text{ cm}^2/\text{g}$  for  $\text{Gd}_2\text{O}_2\text{S:Tb}$  and  $\sigma = 34\text{ cm}^2/\text{g}$ , and  $\tau = 825\text{ cm}^2/\text{g}$  for  $\text{ZnSCdS:Ag}$ .

### 3. Results and discussion

Fig. 2 shows the primary photon component of the detector optical quantum gain, expressed as a function of incident photon energy. Data shown were calculated using Eqs. (1) and (2), i.e. taking into account only radiation photons included in the mass-energy absorption coefficient ( $(\mu/\rho)_{\text{tot, en}}$ ). The coating thickness of scintillators was  $70\text{ mg/cm}^2$ . The shape of curves reflects the combined effect of radiation absorption, optical photon generation, and emission processes within the two materials. As expected, the optical quantum gain shows a sudden increase at the K-edge energy. At 50.2 keV,  $\text{Gd}_2\text{O}_2\text{S:Tb}$  quantum gain increases by approximately 145 optical photons per X-ray. This amounts to 37% of the maximum gain value at the K-edge. For  $\text{ZnSCdS:Ag}$ , at 26.7 keV, the corresponding increase was 56 photons (a gain of about 15%). This behaviour follows the variation of the energy absorption coefficient. For instance, at 50.2 keV the initial value of the  $\text{Gd}_2\text{O}_2\text{S}$  mass-energy absorption coefficient is  $2.625\text{ cm}^2/\text{g}$ , suddenly increasing to  $4.677\text{ cm}^2/\text{g}$  (a 40% increase) and then slowly reducing to 3.946 and  $2.453\text{ cm}^2/\text{g}$  at 60 and 80 keV, respectively (Hubbell, 1995). For energies above the K-edge, X-ray absorption within the scintillator gradually decreases with energy, and hence, energy deposition within the scintillator, light generation and light emission are reduced. Similar considerations also hold for  $\text{ZnSCdS:Ag}$ . It is worth noting that  $\text{ZnSCdS:Ag}$  provides superior performance to  $\text{Gd}_2\text{O}_2\text{S:Tb}$  in the energy interval from about 35 to 50 keV, often used in mammography.

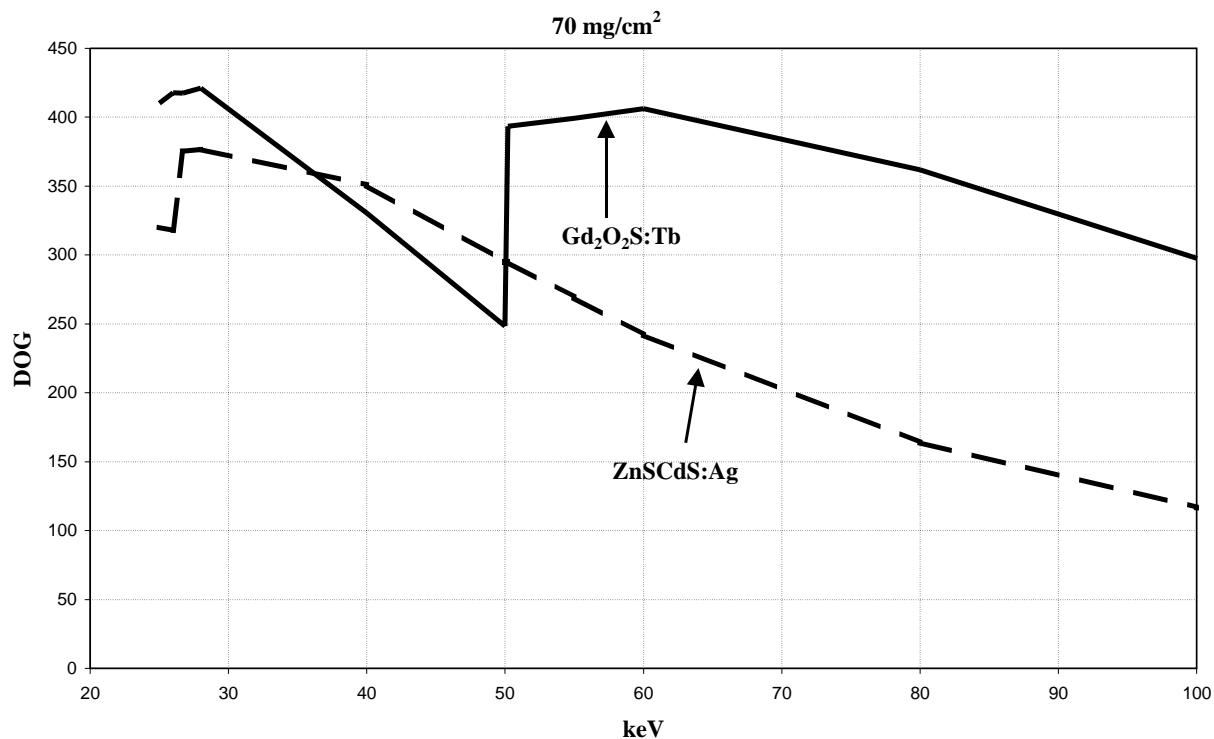


Fig. 2. Variation of detector optical quantum gain (without account of K-fluorescence) with incident photon energy.

Fig. 3 shows the variation with energy of two parameters: (i) The probability for generating a K-characteristic radiation photon per absorbed primary radiation photon (PKA), and (ii) the probability for generating K-characteristic radiation per incident primary radiation photon (PKI). PKI was calculated by Eq. (5). PKA was determined by assuming that all primary incident photons are absorbed. PKA shows a rather slow decrease with X-ray energy for both scintillators under consideration. Although Gd has a higher fluorescence yield (0.932) than Cd (0.8415) (Hubbell et al., 1984), PKA is higher for ZnSCdS for energies up to 200 keV. This is principally due to the significantly higher  $[\mu_p(E, Z)/\mu_T(E)]$  ratio of ZnSCdS with respect to that of Gd<sub>2</sub>O<sub>2</sub>S. This ratio decreases with energy, the values for ZnSCdS ranging from 1.65 at 26.7 keV and 1.77 at 30 keV to 0.828 at 200 keV. On the other hand, for Gd<sub>2</sub>O<sub>2</sub>S the values range from 1.16, at 50 keV, to 0.87 at 200 keV. Additionally Cd has a higher  $f_K$  value (relative contribution of the K-shell to the photoelectric effect):  $f_K = 0.841$  for Cd compared to  $f_K = 0.818$  for Gd (Storm and Israel, 1970). For energies up to 90 keV, the heavy element fractional weights are approximately equal for the two materials. PKA values of ZnSCdS start from 0.57 and remain higher than 0.50 at 80 keV, i.e. well above the K-edge energy of Cd at 26.7 keV. Gd<sub>2</sub>O<sub>2</sub>S also shows a very slight variation—

from 0.36 to 0.24—in the energy range from 50.2 to 250 keV. It is obvious that the shape of the curves in Fig. 3 is governed by the variation of  $\mu_p(E, Z)/\mu_T(E)$ , i.e. the variation of the relative probability of the photoelectric effect over the total photon attenuation probability. It is of interest to compare PKA results with PKI, also shown in Fig. 3. In contrast to PKA, the probability of K-characteristic radiation generation per incident photon decreases rather rapidly with energy. ZnSCdS has a peak value of 0.48 at 26.7 keV, decreases to 0.18 at 50 keV and then further to 0.03 at 100 keV. Gd<sub>2</sub>O<sub>2</sub>S shows a peak value (0.23) at 50.2 keV and exceeds the values of ZnSCdS at higher energies. This is due to the higher incident X-ray attenuation efficiency of Gd<sub>2</sub>O<sub>2</sub>S, which shows higher attenuation coefficient values than ZnSCdS in the whole energy range above 50.2 keV.

Fig. 4 shows the K-photon component of quantum gain, due to K-fluorescence radiation absorption (K\_DOG), and the total gain (TOTAL\_DOG), due to both primary photons (see Fig. 2) and K-fluorescence secondary photons. All curves shown correspond to a coating thickness of 70 mg/cm<sup>2</sup>. Data on K\_DOG were calculated using relation (9). It is of interest to note that, in comparison with Fig. 2, ZnSCdS:Ag is significantly higher than Gd<sub>2</sub>O<sub>2</sub>S:Tb in the range between 27 and 50 keV, since in this range the Gd<sub>2</sub>O<sub>2</sub>S:Tb contribution

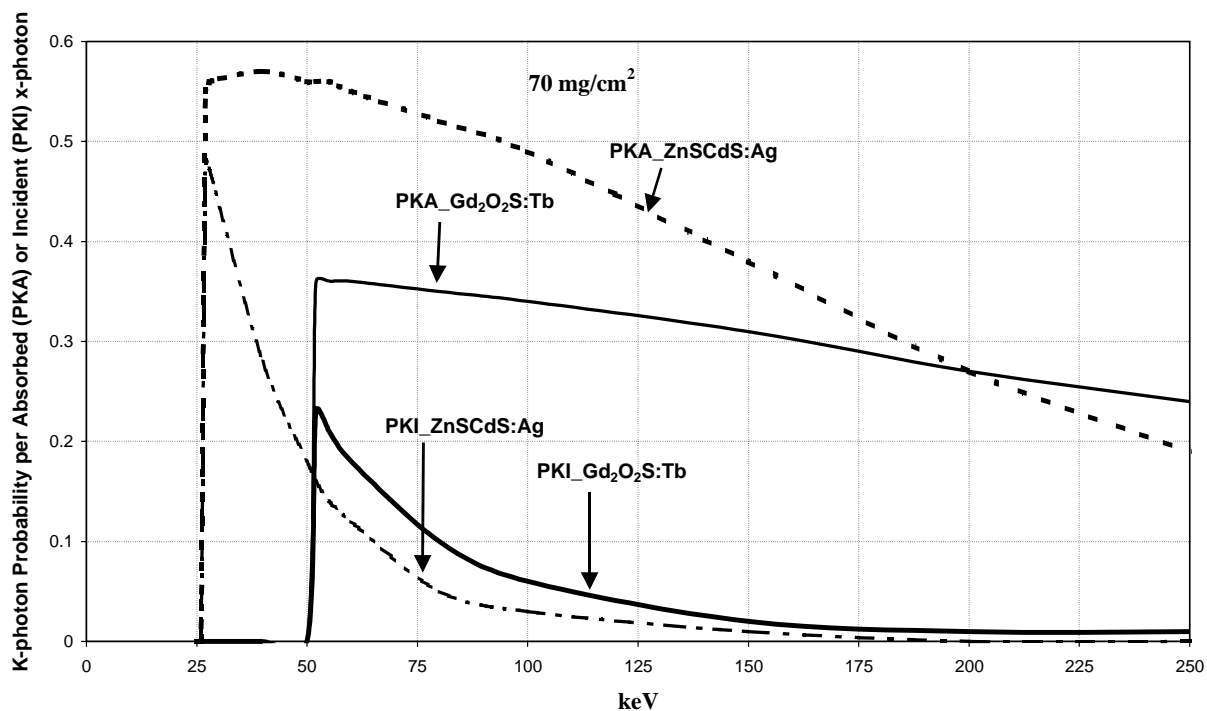


Fig. 3. Probability for generating a K-characteristic radiation photon per absorbed primary radiation photon (PKA), or per incident primary radiation photon (PKI), as a function of incident photon energy.

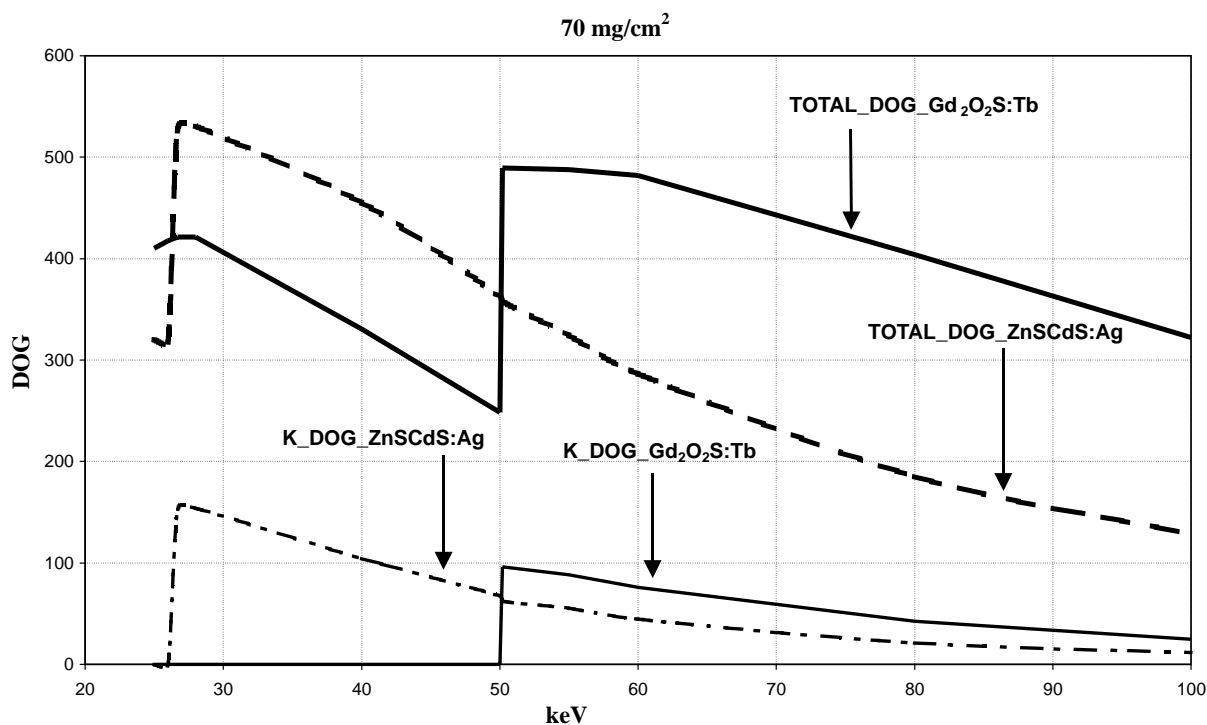


Fig. 4. K-photon component of quantum gain (K.DOG) and total gain (TOTAL.DOG).

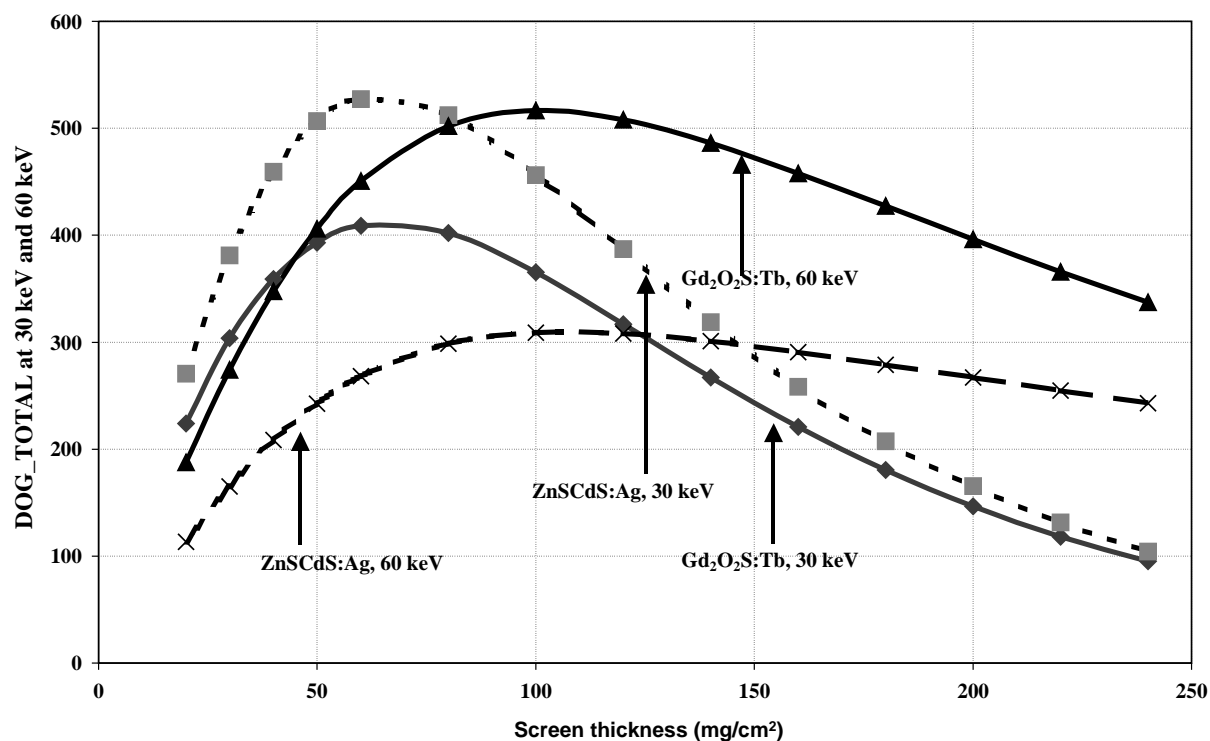


Fig. 5. Variation of detector quantum gain with coating thickness.

to the total DOG values is nil. This range is useful for various X-ray-imaging applications. Additionally, the gain due to secondary K-radiation absorption contributes a significant portion to the overall detector gain. For  $\text{Gd}_2\text{O}_2\text{S}$ , just above the K-edge energy of Gd (50.2 keV), this fraction is of the order of 20% reducing to 8% at 100 keV. For ZnSCdS the corresponding fraction, at 26.7 keV, is approximately 29%, reducing to 9% at 100 keV. It is of interest to note that the maximum value of the total gain of ZnSCdS:Ag (528 photons at 26.7 keV) is higher than that for  $\text{Gd}_2\text{O}_2\text{S:Tb}$  (489 photons at 50.2 keV). Our data on  $\text{Gd}_2\text{O}_2\text{S:Tb}$  are of the same order of magnitude as experimental data, published by Dick and Motz (1981).

The variation of detector quantum gain with coating thickness is illustrated in Fig. 5. Data for  $\text{Gd}_2\text{O}_2\text{S:Tb}$  were obtained at 60 keV, while data for ZnSCdS:Ag were obtained at 30 keV, these energy values being just above the respective K-edge energies. For  $\text{Gd}_2\text{O}_2\text{S:Tb}$  the quantum gain attains a peak value at approximately 100 mg/cm<sup>2</sup> while for ZnSCdS:Ag a peak gain was attained at 60 mg/cm<sup>2</sup>. Since for higher incident photon energies, thicker scintillator layers are necessary in order to absorb the same fraction of incident photons, peak DOG values would also be observed at higher thicknesses.

In conclusion, the theoretical model described in this paper provides a depiction of the physical processes

involved in the detection of radiation during X-ray imaging applications involving use of granular phosphors. This model can predict the overall gain performance of scintillators at various X-ray energies and various coating thicknesses, provided that the values of a number of physical parameters are given. These are: (1) the X-ray attenuation and absorption coefficients, conveniently calculated from tabulated data, (2) the intrinsic X-ray to light conversion efficiency, either available in the literature for a large number of scintillators or conveniently calculated from available intrinsic physical data (the energy band gap of the material, the mean energy of emitted optical photons and other physical parameters), and (3) the optical attenuation coefficients, which depend on the particular light wavelength and grain size and which may be estimated to an acceptable approximation from emission spectrum data, often available in the literature.

## Appendix A

### A.1. Probability of generation and absorption of a K-characteristic fluorescence photon

The probability,  $p_{Fy}^i$ , of generating a K-fluorescence photon in the  $i$ th layer of the scintillator, after the

incidence of one radiation photon of energy  $E$ , may be written as (Chan and Doi, 1983; Kalivas et al., 1999b)

$$p_{F_y}^i(E, E_y) = \frac{w_Z [\mu_P(Z, E)/\rho]}{[\mu_T(E)/\rho]} f_K \omega_K I_y \times \left\{ \exp \left[ -\frac{\mu_T(E)}{\rho} (i-1) \rho_p \Delta L \right] - \exp \left[ -\frac{\mu_T(E)}{\rho} i \rho_p \Delta L \right] \right\}, \quad (\text{A.1})$$

where the index  $y$  denotes either  $\alpha$  or  $\beta$ , signifying that the generated K-fluorescent photon may be either  $K_\alpha$  or  $K_\beta$  X-ray fluorescent photon,  $w_Z$  is the fractional weight of the highest atomic number ( $Z$ ) chemical element in the scintillator, also exhibiting the highest cross section for photoelectric interactions,  $[\mu_P(Z, E)/\rho]$  is the total photoelectric mass attenuation coefficient, at energy  $E$ , for the highest  $Z$  element,  $[\mu_T(E)/\rho]$  is the total mass attenuation coefficient of the scintillator material at energy  $E$ ,  $f_K$  is a factor expressing the relative contribution of the K-shell photoelectric cross section ( $\tau_K$ ) to the total photoelectric effect cross section ( $\tau_K/\tau$ ),  $\omega_K$  is the K-fluorescence yield of the highest  $Z$  element, expressing the probability of K-fluorescence production (i.e. excluding the probability of Auger electron production),  $I_y$  is the relative frequency of either  $K_\alpha$  or  $K_\beta$  fluorescence X-ray photon production (Hubbell et al., 1994) and,  $\rho_p$  is the packing density of the scintillator, i.e. the active scintillator mass per unit of layer volume; for layers containing scintillating grains embedded in a binding medium, packing density is approximately half the active material density (Arnold, 1979). The first factor in expression (A.1), i.e. the ratio containing the photon interaction coefficients and the fractional weight, expresses the probability for photoelectric interaction with the highest  $Z$  element. The factor in brackets gives the attenuation of incident radiation within the  $i$ th layer.

The probability of a K-fluorescence X-ray photon, generated at the  $i$ th scintillator layer and emitted into a solid-angle element  $\Delta\Omega_j$ , interacting at the  $e$ th layer, may be written as

$$p_{A_j}^{i,e}(E_y, \Delta\Omega_j) = \frac{\Delta\Omega_j}{4\pi} \left\{ \exp \left[ -\frac{[\mu_T(E_y)/\rho] (|e-i|-1) \rho_p \Delta L}{|\cos(j-1/2)\Delta\xi|} \right] - \exp \left[ -\frac{[\mu_T(E_y)/\rho] (|e-i)\rho_p \Delta L}{|\cos(j-1/2)\Delta\xi|} \right] \right\}, \quad (\text{A.2})$$

where the solid-angle element  $\Delta\Omega_j$  may be calculated as follows:

$$\Delta\Omega_j = \int_{(j-1)\Delta\xi}^{j\Delta\xi} \frac{2\pi r^2 \sin \phi \, d\phi}{r^2} = 2\pi [\cos(j-1)\Delta\xi - \cos j\Delta\xi], \quad (\text{A.3})$$

where  $\phi$  denotes the semi-angle of the cone subtended at the point of K-characteristic X-ray fluorescence emission (Fig. 1),  $\Delta\xi_j$  is the polar angle element correspond-

ing to the solid-angle element  $\Delta\Omega_j$  and  $r$  is the radius of a sphere centred at the point of emission. The factor in brackets in (A.2) expresses the interaction of K-fluorescence photons within the  $e$ th layer.

The probability of generation and absorption of a K-characteristic fluorescence photon, within the whole scintillator, is obtained after summation over all elementary thin layers  $i$  and  $e$  and also over the solid-angle elements  $j$ , as follows:

$$p_{A,F}^I(E_y) = \sum_{i=1}^I p_{F_y}^i(E, E_y) \sum_{e=1}^I \sum_{j=1}^J p_{A_j}^{i,e}(E_y, \Delta\Omega_j). \quad (\text{A.4})$$

### A.2. The function $\bar{\phi}_\lambda$

This function has been defined as a solution to a photon diffusion differential equation (Swank, 1973), which describes the propagation of light through optical scattering media, and it is given as follows:

$$\bar{\phi}_\lambda(\sigma, \tau, i\Delta L) = \frac{\tau \rho_1 [(\sigma + \tau \rho_0) e^{\sigma i \Delta L} + (\sigma - \tau \rho_0) e^{-\sigma i \Delta L}]}{(\sigma + \tau \rho_0)(\sigma + \tau \rho_1) e^{\sigma L_0} - (\sigma - \tau \rho_0)(\sigma - \tau \rho_1) e^{-\sigma L_0}}, \quad (\text{A.5})$$

where  $\sigma$  is the reciprocal of the optical photon diffusion length, expressing the light attenuation within the scintillator (Hamaker, 1947; Ludwig, 1971; Swank, 1973). According to Swank,  $\sigma$  in (A.5) is identical to the parameter  $\sigma$  used in the one-dimensional Hamaker–Ludwig radiation transport model (Hamaker, 1947; Ludwig, 1971). This parameter is given as a function of the optical scattering and optical absorption coefficients (Ludwig, 1971):

$$\sigma = [\lambda_A (\lambda_A + 2\lambda_S)]^{1/2}, \quad (\text{A.6})$$

$\tau$  being the reciprocal optical relaxation length, which may also be expressed as a function of the optical scattering and absorption coefficients (Ludwig, 1971):

$$\tau = \lambda_A + 2\lambda_S \quad (\text{A.7})$$

with  $\rho_0, \rho_1$  optical parameters which express the reflection of light at the front and back scintillator surfaces, defined as

$$\rho_n = (1 - r_n)/(1 + r_n), \quad n = 0, 1, \quad (\text{A.8})$$

where  $r_n$  denotes the optical reflection coefficients at the front (0) and back (1) screen surfaces.

### A.3. The function $\bar{\phi}_Q(E, w)$

This function is expressed by the equation

$$\bar{\phi}_Q(E, L_0) = \frac{\mu(E) \exp[-\mu(E) i \Delta L] \Delta L}{\sum_{i=1}^I \mu(E) \exp[-\mu(E) i \Delta L] \Delta L}, \quad (\text{A.9})$$

where  $\mu(E)$  is the X-ray absorption coefficient calculated as described above for the quantum detection efficiency  $\bar{\eta}$ . The numerator in Eq. (A.9) gives the probability of X-ray photon absorption at depth  $L = i\Delta L$ . The denominator is equal to the total probability of absorption in a scintillator of thickness  $L_0$ .

## References

- Alig, R., Bloom, S., 1977. Cathodoluminescent efficiency. *J. Electrochem. Soc.* 124 (7), 1136–1138.
- Arnold, B.A., 1979. Physical characteristics of screen-film combinations. In: Haus, A.G. (Ed.), *The Physics of Medical Imaging: Recording System, Measurements and Techniques*. American Association of Physicists in Medicine, New York, pp. 30–71.
- Bartram, R.H., Lempicki, A., 1996. Efficiency of electron-hole pair production in scintillators. *J. Lumin.* 68, 225–240.
- Besch, H.J., 1998. Radiation detectors in medical and biological applications. *Nucl. Instrum. Methods Phys. Res. A* 419, 201–216.
- Bevington, P., 1969. *Data Reduction and Error Analysis for the Physical Sciences*. McGraw-Hill, Maidenhead, NY.
- Blasse, G., 1994. The luminescence efficiency of scintillators for several applications: state-of-the-art. *J. Lumin.* 60&61, 930–935.
- Chan, H.P., Doi, K., 1983. Energy and angular dependence of X-ray absorption and its effect on radiographic response in screen-film systems. *Phys. Med. Biol.* 28 (5), 565–579.
- Curry, T.S., Dowdey, J.E., Murry, R.C., 1990. Luminescent screens. In: Lea, Febiger (Eds.), *Christensen's Physics of Diagnostic Radiology*. London, pp.118–136.
- De Poorter, J.A., Bril, A., 1975. Absolute X-ray efficiencies of some phosphors. *J. Electrochem. Soc.* 122 (8), 1086–1088.
- Dick, C.E., Motz, J.W., 1981. Utilization of monoenergetic X-ray beams to examine the properties of radiographic intensifying screens. *IEEE Trans. Nucl. Sci.* NS-28, 1554–1558.
- Evans, R.D., 1955. *The Atomic Nucleus*. McGraw-Hill, New York, pp. 600–712.
- Groenhuis, R.A., Ferwerda, H.A., Ten Bosch, J.J., 1983. Scattering and absorption of turbid materials determined from reflection measurements. I. Theory. *Appl. Opt.* 22 (16), 2456–2462.
- Hamaker, H., 1947. Radiation and heat conduction in light-scattering material. *Philips Res. Rep.* 2, 55–67.
- Hell, E., Knüpfer, W., Mattern, D., 2000. The evolution of scintillating medical detectors. *Nucl. Instrum. Methods Phys. Res. A* 454, 40–48.
- Hubbell, J.H., 1999. Review of photon interaction cross sections data in the medical and biological context. *Phys. Med. Biol.* 44, R1–R22.
- Hubbell, J.H., Trehan, P.N., Singh, N., Chand, B., Mehta, D., Garg, M.L., Garg, R.R., Singh, S., Puri, S., 1994. A review, bibliography, and tabulation of K, L, and higher atomic shell X-ray fluorescence yields. *J. Phys. Chem. Ref. Data* 23 (2), 339–364.
- Hubbell, J.H., Seltzer, S.M., 1995. Tables of X-ray mass attenuation coefficients and mass energy absorption coefficients 1 to 20 MeV for elements Z=1 to 92 and 48 additional substances of dosimetric interest. US Department of commerce, NISTIR 5632.
- Ishimaru, A., 1989. Diffusion of light in turbid material. *Appl. Opt.* 28 (12), 2210–2215.
- Kalivas, N., Costaridou, L., Kandarakis, I., Cavouras, D., Nomicos, C.D., Panayiotakis, G.S., 1999a. Effect of intrinsic gain fluctuations on quantum noise of phosphor materials used in medical X-ray imaging. *Appl. Phys. A* 69, 337–341.
- Kalivas, N., Kandarakis, I., Cavouras, D., Costaridou, L., Nomicos, C.D., Panayiotakis, G.S., 1999b. Modeling quantum noise of phosphors used in medical X-ray imaging detectors. *Nucl. Instrum. Methods Phys. Res. A* 430, 559–569.
- Kandarakis, I., Cavouras, D., Panayiotakis, G.S., Nomicos, C.D., 1997. Evaluating X-ray detectors for radiographic applications: a comparison of ZnSCdS:Ag with Gd<sub>2</sub>O<sub>2</sub>S:Tb and Y<sub>2</sub>O<sub>2</sub>S:Tb screens. *Phys. Med. Biol.* 42, 1351–1373.
- Kandarakis, I., Cavouras, D., 2001a. Modeling the effect of light generation and light attenuation properties on the performance of phosphors used in medical imaging radiation detectors. *Nucl. Instrum. Methods Phys. Res. A* 460, 412–423.
- Kandarakis, I., Cavouras, D., 2001b. Role of the activator in the performance of scintillators used in X-ray imaging. *Appl. Rad. Isot.* 54, 821–831.
- Kandarakis, I., Cavouras, D., 2001c. Experimental and theoretical assessment of the performance of Gd<sub>2</sub>O<sub>2</sub>S:Tb and La<sub>2</sub>O<sub>2</sub>S:Tb phosphors and Gd<sub>2</sub>O<sub>2</sub>S-La<sub>2</sub>O<sub>2</sub>S:Tb mixtures for X-ray imaging. *Eur. Radiol.* 11, 1083–1091.
- Knoll, F.G., 1989. *Radiation Detection and Measurement*. Wiley, New York, 54pp.
- Lindström, J., Carlsson, G.A., 1999. A simple model for estimating the particle size dependence of absolute efficiency of fluorescent screens. *Phys. Med. Biol.* 44, 1353–1360.
- Ludwig, G.W., 1971. X-ray efficiency of powder phosphors. *J. Electrochem. Soc.* 118 (7), 1152–1159.
- Lumilux Data Book, 1989. Riedel-de-Haen, Seelze, Germany.
- Morlotti, R., 1975. X-ray efficiency and modulation transfer function of fluorescent rare earth screens, determined by the Monte-Carlo method. *J. Photogr. Sci.* 33, 181–189.
- Ning, R., Chen, B., Yu, R., Conover, D., Tang, X., Ning, Y., 2000. Flat panel detector-based cone-beam volume ct angiography: system evaluation. *IEEE Trans. Med. Imag.* 19 (9), 949–963.
- Nishikawa, R.M., Yaffe, M.J., 1990. Model of the spatial-frequency-dependent detective quantum efficiency of phosphor screens. *Med. Phys.* 17, 894–904.
- Phillips, W., Stanton, M., Xie, J., O' Mara, D., Kalata, K., 1993. A CCD-based area detector for crystallography using synchrotron and laboratory sources. *Nucl. Instrum. Methods Phys. Res. A* 334, 621–630.
- Press, W.H., Flannery, B.P., Teukolsky, S.A., Vetterling, W.T., 1990. *Numerical Recipes in C: The Art of Scientific Computing*. Cambridge University Press, Cambridge, pp.540–547.
- Storm, E., Israel, H., 1967. Photon cross-sections from 0.001 to 100 MeV for elements 1 through 100. Report LA-3753, Los

- Alamos Scientific Laboratory of the University of California.
- Swank, R.K., 1973. Calculation of modulation transfer functions of X-ray fluorescent screens. *Appl. Opt.* 12 (8), 1865–1870.
- Van de Hulst, H.C., 1957. In: *Light Scattering by Small Particles*. Willey, New York, pp. 103–107.
- Zurro, B., Ibarra, A., Mc Carthy, K.J., Acuna, A.U., Sastre, R., 1995. Comparison of phosphors for broadband plasma emission detectors. *Rev. Sci. Instrum.* 66, 534–536.
- Zweig, G., Zweig, D.A., 1983. Radioluminescent imaging: factors affecting total light output. *Proc. SPIE* 419, 297–304.